12

DQ analysis of 2D and 3D natural convection in an inclined cavity using a velocity-vorticity formulation

D. C. Lo*
*Institute of Navigation Science and Technology, National Kaohsiung Marine University, Kaohsiung, Taiwan. E-mail:loderg@mail.nkmu.edu.tw

1. Introduction

Computation of incompressible Navier-Stokes equations is an important area in CFD related fields in science and engineering. With the development of a wide range of numerical schemes and algorithms, obtaining numerical solution of the Navier-Stokes equations now has become much easier compared to the previous decades. However, there is a continuous research going on in the development of new numerical algorithms as the CFD is being used as a modeling tool in other areas of science as well. The velocity-vorticity formulation, pioneered by Fasel (1976) is considered to be an alternate form of the Navier-Stokes equations without involving the pressure term.

Generally the vorticity boundary values are determined explicitly using a second order accurate Taylor's series expansion scheme while computing flow fields using the velocity-vorticity form of the Navier-Stokes equations. Hence care must be taken to assure accurate computation of the vorticity values at the boundaries by using finer mesh near the boundaries when lower order schemes are used for vorticity definition. The use of the differential quadrature method enables the computation of vorticity definition with higher order polynomials. Furthermore, when a coupled numerical scheme involving a global method of differential quadrature (DQ) method is used to solve the governing equations, the explicit specification of vorticity definition at the boundary is completely eliminated, resulting in a simplified computational procedure.

Bellman et al. (1972) developed the DQ method to approximate the derivative of a smooth function and has been successfully implemented for solving many engineering problems. Shu and Richards (1992) applied a generalized differential quadrature for the simulation of 2D incompressible viscous flow simulation. Shu (2000) reported an elaboration of the differential quadrature method. Additionally, Lo et al. (2005) applied a differential quadrature method to solve 2D and 3D natural convection problems in a differentially heated enclosure by velocity-vorticity formulation. The present study proposes a novel idea to solve 2D and 3D Navier-Stokes equations by efficiently exploiting the advantages of both the velocity-vorticity form of the Navier-Stokes equations and the DQ method. Natural convection in a differentially heated inclined cubic cavity is represented by continuity

equation, momentum equations and energy equation, which are coupled due to the buoyancy term appearing in the momentum equation. Hence natural convection in an inclined cubic cavity is considered to be the suitable example problem to test the numerical capability of the proposed coupled algorithm.
The proposed numerical scheme is applied to determine the velocity, vorticity and temperature variations for natural convection problem in a differentially heated inclined cavity for Rayleigh number range from 10^3 to 10^6 . Numerical formulation, solution procedure and comparisons of the present results with those obtained by other numerical schemes are presented in the following sections.

2. Differential quadrature method

The DQ method replaces a given spatial derivative of a function $f(x)$ by a linear weighted sum of the function values at the discrete sample points considered along a coordinate direction, resulting in a set of algebraic equations. Hence the DQ method can be used to obtain numerical solution of partial differential equations with higher order accuracy. For a function of three variables $f(x, y, z)$, the p th order derivatives, q th order derivatives and r th order derivatives of the function with respect to x , y and z coordinates can be obtained as:

$$f_x^{(p)}(x_i, y_j, z_k) = \sum_{l=1}^{L} A_{i,l}^{(p)} f(x_l, y_j, z_k), p = 1,2,...,L-1 \tag{1}$$

$$f_y^{(q)}(x_i, y_j, z_k) = \sum_{m=1}^{M} B_{j,m}^{(q)} f(x_i, y_m, z_k), q = 1,2,...,M-1 \tag{2}$$

$$f_z^{(r)}(x_i, y_j, z_k) = \sum_{n=1}^{N} C_{k,n}^{(r)} f(x_i, y_j, z_n), r = 1,2,...,N-1 \tag{3}$$

for $i = 1,2,...,L; \quad j = 1,2,...,M; \quad k = 1,2,...,N$
where l , m , n are the indices for the grid points in the x , y and z coordinates respectively, L, M, N are the number of grid points in the x , y and z directions respectively and $A_{i,l}^{(p)}, B_{j,m}^{(q)}, C_{k,n}^{(r)}$ are the weighting coefficients. The first order weighting coefficients $A_{i,l}^{(1)}, B_{j,m}^{(1)}, C_{k,n}^{(1)}$ can be determined as follows:

$$A_{i,j}^{(1)} = \frac{L^{(1)}(x_i)}{(x_i - x_j)L^{(1)}(x_j)}, i, j = 1,2,...,L, \quad but\ j \neq i \tag{4}$$

$$B_{i,j}^{(1)} = \frac{M^{(1)}(y_i)}{(y_i - y_j)M^{(1)}(y_j)}, i, j = 1,2,...,M, \quad but\ j \neq i \tag{5}$$

$$C_{i,j}^{(1)} = \frac{N^{(1)}(z_i)}{(z_i - z_j)N^{(1)}(z_j)}, i, j = 1,2,...,N, \quad but\ j \neq i \tag{6}$$

where

$$L^{(1)}(x_i) = \prod_{j=1, j\neq i}^{L} (x_i - x_j),$$

$$M^{(1)}(y_i) = \prod_{j=1, j\neq i}^{M} (y_i - y_j),$$

$$N^{(1)}(z_i) = \prod_{j=1, j\neq i}^{N} (z_i - z_j)$$

Similarly the weighting coefficients for the second- and higher-order derivatives can be obtained as

$$A_{i,j}^{(p)} = p(A_{i,i}^{(p-1)} A_{i,j}^{(1)} - \frac{A_{i,j}^{(p-1)}}{x_i - x_j}), i, j = 1, 2, ..., L, \quad but\ j \neq i, l = 2, 3, ..., L-1 \tag{7}$$

$$B_{i,j}^{(q)} = q(B_{i,i}^{(q-1)} B_{i,j}^{(1)} - \frac{B_{i,j}^{(q-1)}}{y_i - y_j}), i, j = 1, 2, ..., M, \quad but\ j \neq i, m = 2, 3, ..., M-1 \tag{8}$$

$$C_{i,j}^{(r)} = r(C_{i,i}^{(r-1)} C_{i,j}^{(1)} - \frac{C_{i,j}^{(r-1)}}{z_i - z_j}), i, j = 1, 2, ..., N, \quad but\ j \neq i, n = 2, 3, ..., N-1 \tag{9}$$

It should be noted from the above equations that the weighting coefficients of the second and higher-order derivatives can be computed from the first-order derivatives themselves.

3. Governing equations

The governing equations for natural convection can be described by the incompressible Navier-Stokes equations and the energy equation. Assuming the Boussinesq approximation, the velocity-vorticity form of the Navier-Stokes equations can be written in non-dimensional form as follows:

Velocity Poisson

$$\nabla^2 u = -\nabla \times \vec{\omega} \tag{10}$$

Vorticity transport equations

$$\frac{\partial \vec{\omega}}{\partial t} + (\vec{v} \cdot \nabla)\vec{\omega} = (\vec{\omega} \cdot \nabla)\vec{v} + Pr \cdot \nabla^2 \vec{\omega} - Ra \Pr \nabla \times T\vec{g} \tag{11}$$

Energy equation

$$\frac{\partial T}{\partial t} + (\vec{v} \cdot \nabla)T = \nabla^2 T \tag{12}$$

The computational domain is discretized using a Cartesian coordinate frame with $x - y$ representing the horizontal plane and z directing in the vertical direction. In the velocity-vorticity form of the Navier-Stokes equations, the vorticity vector is defined as

$$\vec{\omega} = \nabla \times \vec{u} \tag{13}$$

Equations (10-12) are the final form of the governing equations that characterize the flow and heat transfer during a natural convection process. These equations have to be solved in a computational domain Ω which is enclosed by a solid boundary Γ. For the problem of natural convection in a differentially heated cubic cavity, no-slip velocity boundary conditions are assumed on all the boundary walls.

4. Numerical solution

Application of the DQ method to spatial discretization of the governing equations results in a set of algebraic equations. For example, the velocity Poisson equation in the $x-$ direction is approximated using the DQ method to obtain the velocity component in the one coordinate direction as follows,

$$\sum_{l=1}^{L} A_{i,l}^{(2)} u_{l,j,k} + \sum_{m=1}^{M} B_{j,m}^{(2)} u_{i,m,k} + \sum_{n=1}^{N} C_{k,n}^{(2)} u_{i,j,n} + \sum_{m=1}^{M} B_{j,m}^{(1)} \zeta_{i,m,k} - \sum_{n=1}^{N} C_{k,n}^{(1)} \eta_{i,j,n} = 0 \tag{14}$$

Similarly, the velocity components in the $y-$, $z-$ directions also can be used the same formulas.

The time derivatives of the convection-diffusion equation (vorticity transport equations and energy equation) are discretized using a second order accurate three-time-level scheme expressed as

$$\begin{aligned} &\frac{\partial \phi}{\partial t} + \vec{v} \cdot \nabla \phi = \nabla^2 \phi + f \Rightarrow \\ &\frac{3\phi^{t+1} - 4\phi^{t} + \phi^{t-1}}{2\Delta t} + 2\vec{v}^{\,t} \cdot \nabla \phi^{t} - \vec{v}^{\,t-1} \cdot \nabla \phi^{t-1} = \nabla^2 \phi^{t+1} + f^{t+1} \end{aligned} \tag{15}$$

The convection-diffusion equation (15) is approximated by the DQ method as follows:

$$\begin{aligned} &\frac{(3\phi_{i,j,k}^{t+1})}{2\Delta t} - (\sum_{l=1}^{L} A_{i,l}^{(2)} \phi_{l,j,k} + \sum_{m=1}^{M} \phi_{j,m}^{(2)} \xi_{i,m,k} + \sum_{n=1}^{N} C_{k,n}^{(2)} \phi_{i,j,n})^{t+1} - (f_{i,j,k}^{t+1}) \\ &= \frac{(4\phi_{i,j,k}^{t})}{2\Delta t} - \frac{(\phi_{i,j,k}^{t-1})}{2\Delta t} - 2(u_{i,j,k} \sum_{l=1}^{L} A_{i,l}^{(1)} \phi_{l,j,k} + v_{i,j,k} \sum_{m=1}^{M} B_{j,m}^{(1)} \phi_{i,m,k} + w_{i,j,k} \sum_{n=1}^{N} C_{k,n}^{(1)} \phi_{i,j,n})^{t} \\ &+ (u_{i,j,k} \sum_{l=1}^{L} A_{i,l}^{(1)} \phi_{l,j,k} + v_{i,j,k} \sum_{m=1}^{M} B_{j,m}^{(1)} \phi_{i,m,k} + w_{i,j,k} \sum_{n=1}^{N} C_{k,n}^{(1)} \phi_{i,j,n})^{t-1} \end{aligned} \tag{16}$$

Combining equations (10) to (12), all the seven field variables can be represented by means of a single global matrix as:

$$\begin{bmatrix} A & 0 & 0 & 0 & -D & C & 0 \\ 0 & A & 0 & D & 0 & -B & 0 \\ 0 & 0 & A & -C & B & 0 & 0 \\ 0 & 0 & 0 & E & 0 & 0 & G \\ 0 & 0 & 0 & 0 & E & 0 & H \\ 0 & 0 & 0 & 0 & 0 & E & I \\ 0 & 0 & 0 & 0 & 0 & 0 & F \end{bmatrix} \begin{Bmatrix} u \\ v \\ w \\ \xi \\ \eta \\ \zeta \\ T \end{Bmatrix} = \begin{Bmatrix} f_u \\ f_v \\ f_w \\ f_\xi \\ f_\eta \\ f_\zeta \\ f_T \end{Bmatrix} \tag{17}$$

where the A, B, C, D, E, F, G, H and I are the influence matrices, the $f_u, f_v, f_w, f_\xi, f_\eta, f_\zeta, f_T$ are the loading matrices in the right hand side, the u, v, w are the unknown variables for velocities, ξ, η, ζ are the unknown variables for vorticities, T are the unknown variables. The various differential operators that appear in the DQ approximation equations (10) to (12) and are computed as

$$[A] = \sum_{l=1}^{L} A_{i,l}^{(2)} + \sum_{m=1}^{M} B_{j,m}^{(2)} + \sum_{n=1}^{N} C_{k,n}^{(2)}$$

$$[B] = \sum_{l=1}^{L} A_{i,l}^{(1)}\ ,\ [C] = \sum_{m=1}^{M} B_{j,m}^{(1)}\ ,\ [D] = \sum_{n=1}^{N} C_{k,n}^{(1)}$$

$$[E] = \frac{3}{2\Delta t} - \Pr(\sum_{l=1}^{L} A_{i,l}^{(2)} + \sum_{m=1}^{M} B_{j,m}^{(2)} + \sum_{n=1}^{N} C_{k,n}^{(2)})$$

$$[F] = \frac{3}{2\Delta t} - (\sum_{l=1}^{L} A_{i,l}^{(2)} + \sum_{m=1}^{M} B_{j,m}^{(2)} + \sum_{n=1}^{N} C_{k,n}^{(2)})$$

$$[G] = -Ra \cdot \Pr \cdot \cos\phi \cdot \sum_{m=1}^{M} B_{j,m}^{(1)},$$

$$[H] = Ra \cdot \Pr(\cos\phi \cdot \sum_{l=1}^{L} A_{i,l}^{(1)} - \sin\phi \cdot \sum_{n=1}^{N} C_{k,n}^{(1)})$$

$$[H] = Ra \cdot \Pr(\sin\phi \cdot \sum_{m=1}^{M} B_{j,m}^{(1)})$$

$$[f_u] = 0, [f_v] = 0, [f_w] = 0$$

$$[f_\xi] = \frac{(4\xi_{i,j,k}^{t})}{2\Delta t} - \frac{(\xi_{i,j,k}^{t-1})}{2\Delta t} - 2(u_{i,j,k}\sum_{l=1}^{L} A_{i,l}^{(1)}\xi_{l,j,k} + v_{i,j,k}\sum_{m=1}^{M} B_{j,m}^{(1)}\xi_{i,m,k} + w_{i,j,k}\sum_{n=1}^{N} C_{k,n}^{(1)}\xi_{i,j,n})^{t}$$

$$+(u_{i,j,k}\sum_{l=1}^{L} A_{i,l}^{(1)}\xi_{l,j,k} + v_{i,j,k}\sum_{m=1}^{M} B_{j,m}^{(1)}\xi_{i,m,k} + w_{i,j,k}\sum_{n=1}^{N} C_{k,n}^{(1)}\xi_{i,j,n})^{t-1}$$

$$+2(\xi_{i,j,k}\sum_{l=1}^{L} A_{i,l}^{(1)}u_{l,j,k} + \eta_{i,j,k}\sum_{m=1}^{M} B_{j,m}^{(1)}u_{i,m,k} + \zeta_{i,j,k}\sum_{n=1}^{N} C_{k,n}^{(1)}u_{i,j,n})^{t}$$

$$-(\xi_{i,j,k}\sum_{l=1}^{L} A_{i,l}^{(1)}u_{l,j,k} + \eta_{i,j,k}\sum_{m=1}^{M} B_{j,m}^{(1)}u_{i,m,k} + \zeta_{i,j,k}\sum_{n=1}^{N} C_{k,n}^{(1)}u_{i,j,n})^{t-1}$$

$$[f_\eta]=\frac{(4\eta^{t}_{i,j,k})}{2\Delta t}-\frac{(\eta^{t-1}_{i,j,k})}{2\Delta t}-2(u_{i,j,k}\sum_{l=1}^{L}A^{(1)}_{i,l}\eta_{l,j,k}+v_{i,j,k}\sum_{m=1}^{M}B^{(1)}_{j,m}\eta_{i,m,k}+w_{i,j,k}\sum_{n=1}^{N}C^{(1)}_{k,n}\eta_{i,j,n})^{t}$$
$$+(u_{i,j,k}\sum_{l=1}^{L}A^{(1)}_{i,l}\eta_{l,j,k}+v_{i,j,k}\sum_{m=1}^{M}B^{(1)}_{j,m}\eta_{i,m,k}+w_{i,j,k}\sum_{n=1}^{N}C^{(1)}_{k,n}\eta_{i,j,n})^{t-1}$$
$$+2(\xi_{i,j,k}\sum_{l=1}^{L}A^{(1)}_{i,l}v_{l,j,k}+\eta_{i,j,k}\sum_{m=1}^{M}B^{(1)}_{j,m}v_{i,m,k}+\zeta_{i,j,k}\sum_{n=1}^{N}C^{(1)}_{k,n}v_{i,j,n})^{t}$$
$$-(\xi_{i,j,k}\sum_{l=1}^{L}A^{(1)}_{i,l}v_{l,j,k}+\eta_{i,j,k}\sum_{m=1}^{M}B^{(1)}_{j,m}v_{i,m,k}+\zeta_{i,j,k}\sum_{n=1}^{N}C^{(1)}_{k,n}v_{i,j,n})^{t-1}$$
$$[f_\zeta]=\frac{(4\zeta^{t}_{i,j,k})}{2\Delta t}-\frac{(\zeta^{t-1}_{i,j,k})}{2\Delta t}-2(u_{i,j,k}\sum_{l=1}^{L}A^{(1)}_{i,l}\zeta_{l,j,k}+v_{i,j,k}\sum_{m=1}^{M}B^{(1)}_{j,m}\zeta_{i,m,k}+w_{i,j,k}\sum_{n=1}^{N}C^{(1)}_{k,n}\zeta_{i,j,n})^{t}$$
$$+(u_{i,j,k}\sum_{l=1}^{L}A^{(1)}_{i,l}\zeta_{l,j,k}+v_{i,j,k}\sum_{m=1}^{M}B^{(1)}_{j,m}\zeta_{i,m,k}+w_{i,j,k}\sum_{n=1}^{N}C^{(1)}_{k,n}\zeta_{i,j,n})^{t-1}$$
$$+2(\xi_{i,j,k}\sum_{l=1}^{L}A^{(1)}_{i,l}w_{l,j,k}+\eta_{i,j,k}\sum_{m=1}^{M}B^{(1)}_{j,m}w_{i,m,k}+\zeta_{i,j,k}\sum_{n=1}^{N}C^{(1)}_{k,n}w_{i,j,n})^{t}$$
$$-(\xi_{i,j,k}\sum_{l=1}^{L}A^{(1)}_{i,l}w_{l,j,k}+\eta_{i,j,k}\sum_{m=1}^{M}B^{(1)}_{j,m}w_{i,m,k}+\zeta_{i,j,k}\sum_{n=1}^{N}C^{(1)}_{k,n}w_{i,j,n})^{t-1}$$
$$[f_T]=\frac{(4T^{t}_{i,j,k})}{2\Delta t}-\frac{(T^{t-1}_{i,j,k})}{2\Delta t}-2(u_{i,j,k}\sum_{l=1}^{L}A^{(1)}_{i,l}T_{l,j,k}+v_{i,j,k}\sum_{m=1}^{M}B^{(1)}_{j,m}T_{i,m,k}+w_{i,j,k}\sum_{n=1}^{N}C^{(1)}_{k,n}T_{i,j,n})^{t}$$
$$+(u_{i,j,k}\sum_{l=1}^{L}A^{(1)}_{i,l}T_{l,j,k}+v_{i,j,k}\sum_{m=1}^{M}B^{(1)}_{j,m}T_{i,m,k}+w_{i,j,k}\sum_{n=1}^{N}C^{(1)}_{k,n}T_{i,j,n})^{t-1}$$

where ϕ is the angle of inclination and t is the time level index.

Using the above formula, the vorticity transport equations in the $x-$, $y-$, $z-$ directions and energy equation can be adopted the above method of approximation.

In the successive time step, we used the velocity, vorticity and temperature components at the previous time step as the initial guess for the next iteration. The computations are carried out until steady state conditions are reached. The convergence criteria used in the time loop to achieve steady state conditions are

$$\sqrt{\frac{\sum_{i=1}^{Nodes}(u_i^{t+1}-u_i^{t})}{Nodes-1}}\le 10^{-5},\sqrt{\frac{\sum_{i=1}^{Nodes}(v_i^{t+1}-v_i^{t})}{Nodes-1}}\le 10^{-5},\sqrt{\frac{\sum_{i=1}^{Nodes}(w_i^{t+1}-w_i^{t})}{Nodes-1}}\le 10^{-5}$$
$$\sqrt{\frac{\sum_{i=1}^{Nodes}(\xi_i^{t+1}-\xi_i^{t})}{Nodes-1}}\le 10^{-5},\sqrt{\frac{\sum_{i=1}^{Nodes}(\eta_i^{t+1}-\eta_i^{t})}{Nodes-1}}\le 10^{-5},\sqrt{\frac{\sum_{i=1}^{Nodes}(\zeta_i^{t+1}-\zeta_i^{t})}{Nodes-1}}\le 10^{-5} \quad (18)$$

For the DQ method, the mesh point distribution in the three spatial directions is assumed to be the same and is expressed as

$$x_i = \frac{\cos[\pi/(2L)] - \cos[(2i-1)\pi/(2L)]}{\cos[\pi/(2L)] - \cos[(2L-1)\pi/(2L)]}, \quad i = 1,2,.....,L$$
$$y_j = \frac{\cos[\pi/(2M)] - \cos[(2j-1)\pi/(2M)]}{\cos[\pi/(2M)] - \cos[(2M-1)\pi/(2M)]}, \quad j = 1,2,.....,M \tag{19}$$
$$z_k = \frac{\cos[\pi/(2N)] - \cos[(2k-1)\pi/(2N)]}{\cos[\pi/(2N)] - \cos[(2N-1)\pi/(2N)]}, \quad k = 1,2,.....,N$$

where L, M, N are the number of gird points in the x, y and z directions respectively.

5. Numerical results

Figure 1 shows the schematic diagram of the inclined cubic cavity with the boundary conditions for the natural convection problem. Temperatures equal to –0.5 and 0.5 are enforced on the left wall at $x = -0.5$ and the right wall at $x = 0.5$ respectively. Numerical results obtained for the test problem are discussed in this section.

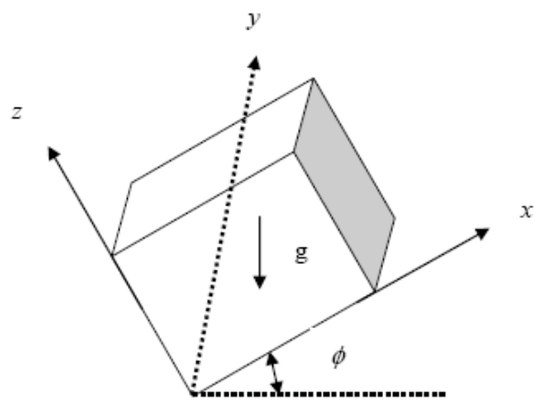

Fig. 1. Layout of the problem

5.1 Grid Independence Study

One of the aims of the present numerical scheme is to show that the use of higher order polynomials for approximating the partial differential equations requires relatively a coarse mesh to achieve benchmark solutions. In order to validate the computer program developed to solve the governing equations for the natural convection problem, initially a grid independence study was carried out for $Ra = 10^4, 10^5, 10^6$.

Further, in order to make sure that the grid independence study is in accordance with other numerical results, the grid independence study results obtained for the case of $\phi = 0°$ were compared with the results of Tric et al. (2000) who used pseudo-spectral Chebyshev algorithm based on the projection-diffusion method with a spatial resolution supplied by polynomial expansions. For the mesh sensitivity study, the mean and the overall Nusselt number values were computed for $10^4 \le Ra \le 10^6$ using four different meshes. The value of Prandtl number was assumed as 0.71 for all these computations. Table 1 depicts the

comparisons between the values of the mean and the overall Nusselt numbers obtained using the present method for the four mesh sizes and the results obtained by Tric et al. (2000). It can be observed that the results obtained by using the present numerical algorithm with the above four grids of size are almost in excellent agreement with the results of Tric et al. (2000) for all the values of the Rayleigh numbers considered in this study. Table 2 shows the 2D and 3D comparison of the mean value and overall value of the Nusselt number for $Ra = 10^3, 10^4, 10^5, 10^6$ at different angles.

Grids	*Nu*	$Ra = 10^4$	$Ra = 10^5$	$Ra = 10^6$
Tric et al. (2000): 81^3 grids	Nu_{mean}	2.251	4.613	8.877
	Nu_{over}	2.054	4.337	8.641
Present: 21^3 grids	Nu_{mean}	2.253	4.624	8.909
	Nu_{over}	2.052	4.329	8.669
Present: 23^3 grids	Nu_{mean}	2.251	4.610	8.910
	Nu_{over}	2.054	4.335	8.668
Present: 25^3 grids	Nu_{mean}	2.251	4.610	8.910
	Nu_{over}	2.054	4.335	8.668
Present: 31^3 grids	Nu_{mean}	2.251	4.610	8.910
	Nu_{over}	2.054	4.335	8.668

Table 1. Grid-independence study results for $Ra = 10^4, 10^5, 10^6$

Ra	Nusselt number	0°	15°	30°	45°	60°	75°	90°
$Ra = 10^3$	2D Nu_{mean}	1.118	1.096	1.069	1.042	1.020	1.025	1.319
	3D Nu_{mean}	1.088	1.073	1.053	1.033	1.016	1.004	1.001
	3D Nu_{over}	1.071	1.059	1.043	1.027	1.013	1.003	1.001
$Ra = 10^4$	2D Nu_{mean}	2.244	2.008	1.709	1.411	1.180	1.047	1.319
	3D Nu_{mean}	2.251	1.986	1.680	1.391	1.172	1.033	1.015
	3D Nu_{over}	2.054	1.843	1.589	1.343	1.152	1.038	1.015
$Ra = 10^5$	2D Nu_{mean}	4.521	3.953	3.028	2.037	1.378	1.082	1.319
	3D Nu_{mean}	4.610	3.969	3.024	2.039	1.384	1.037	1.160
	3D Nu_{over}	4.335	3.773	2.901	1.979	1.362	1.079	1.160
$Ra = 10^6$	2D Nu_{mean}	8.823	7.522	5.323	2.857	1.568	1.120	1.319
	3D Nu_{mean}	8.910	7.545	5.330	2.875	1.583	1.008	1.824
	3D Nu_{over}	8.668	7.363	5.213	2.820	1.558	1.118	1.824

Table 2. 2D and 3D numerical results for $Ra = 10^3, 10^4, 10^5, 10^6$ at different angles

5.2 Effect of Angle of Inclination on Natural Convection Phenomenon References

In order to capture the three-dimensional effect of the temperature fields, the temperature variations on the mid-planes along the principal axes serve as a visual representation of the temperature variations throughout the cavity due to the buoyancy-induced flows. Figures. 2(a) to 2(d) show the temperature contours on $x-z$ plane at $y=0.5$ for different angles of inclination for $Ra=10^5$. As far as the convective heat transport is concerned this is the principal plane that indicates the heat transfer phenomena because this plane consists of the axes of the temperature differentials and the gravitational direction. The temperature maps are very close to the hot and the cold walls compared to the other sides, because greater temperature gradients are observed only at these regions. As the other sides are kept adiabatic, the temperature contours are always normal to these sides as observed in the above figures. Further the increase in the angle of inclination results in diagonally parallel isotherms instead of the nearly horizontal isotherms observed at $\phi=0^\circ$.

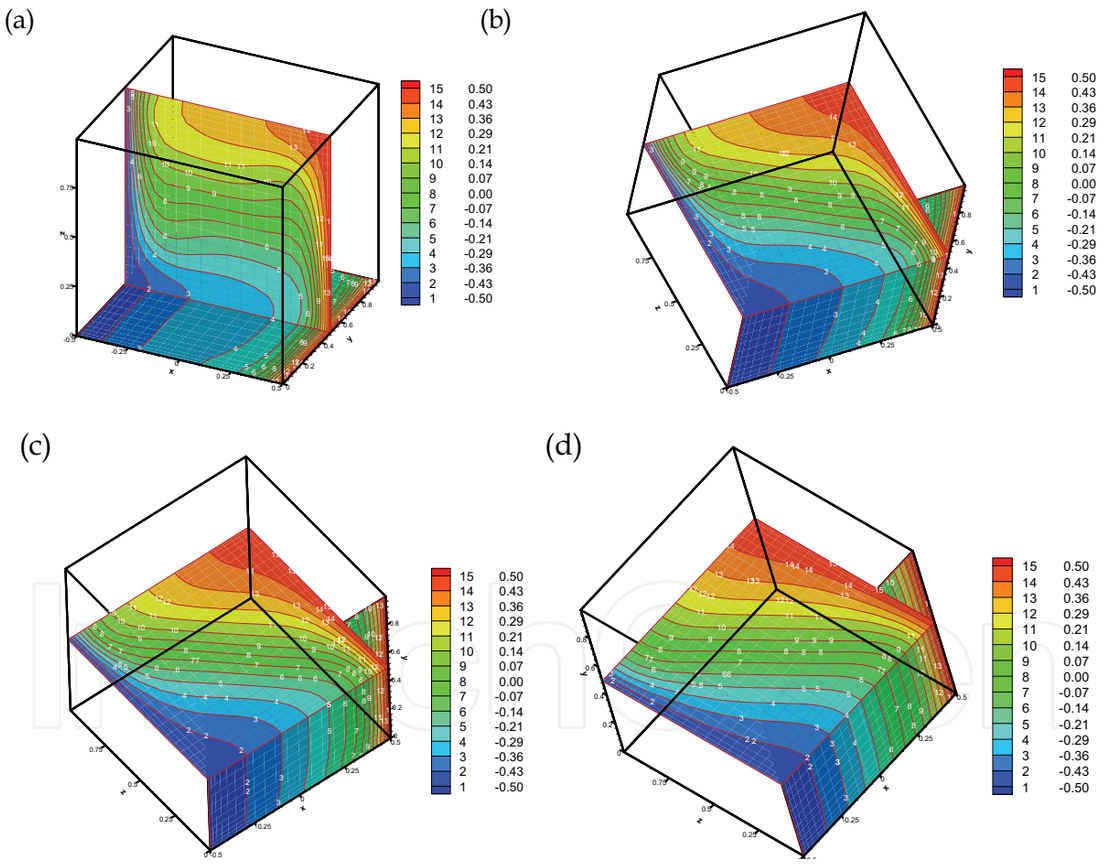

Fig. 2. Temperature contours at $y=0.5$ plane for $Ra=10^5$ in a different angle (a) $\phi=0^0$ (b) $\phi=30^0$ (c) $\phi=45^0$ (d) $\phi=60^0$

Apart from testing the code for the present formulation with respect to the Nusselt numbers, it is also required to verify for the flow fields. The characteristics of the natural convection

phenomenon can be well understood by plotting the velocity vectors on the various symmetric mid-planes along the principal axes. Figures. 3(a) to 3(d) represent the velocity vectors plotted on $x-z$ plane at $y=0.5$ symmetric plane of the cavity for $\phi=0^{\circ},30^{\circ},45^{\circ},60^{\circ}$, respectively at $Ra=10^5$. As the angle of inclination increases the effect of decreased buoyancy forces is felt on the flow pattern. With increase in the angle of inclination, the velocity gradient decreases near the vertical walls as observed in the above figures.

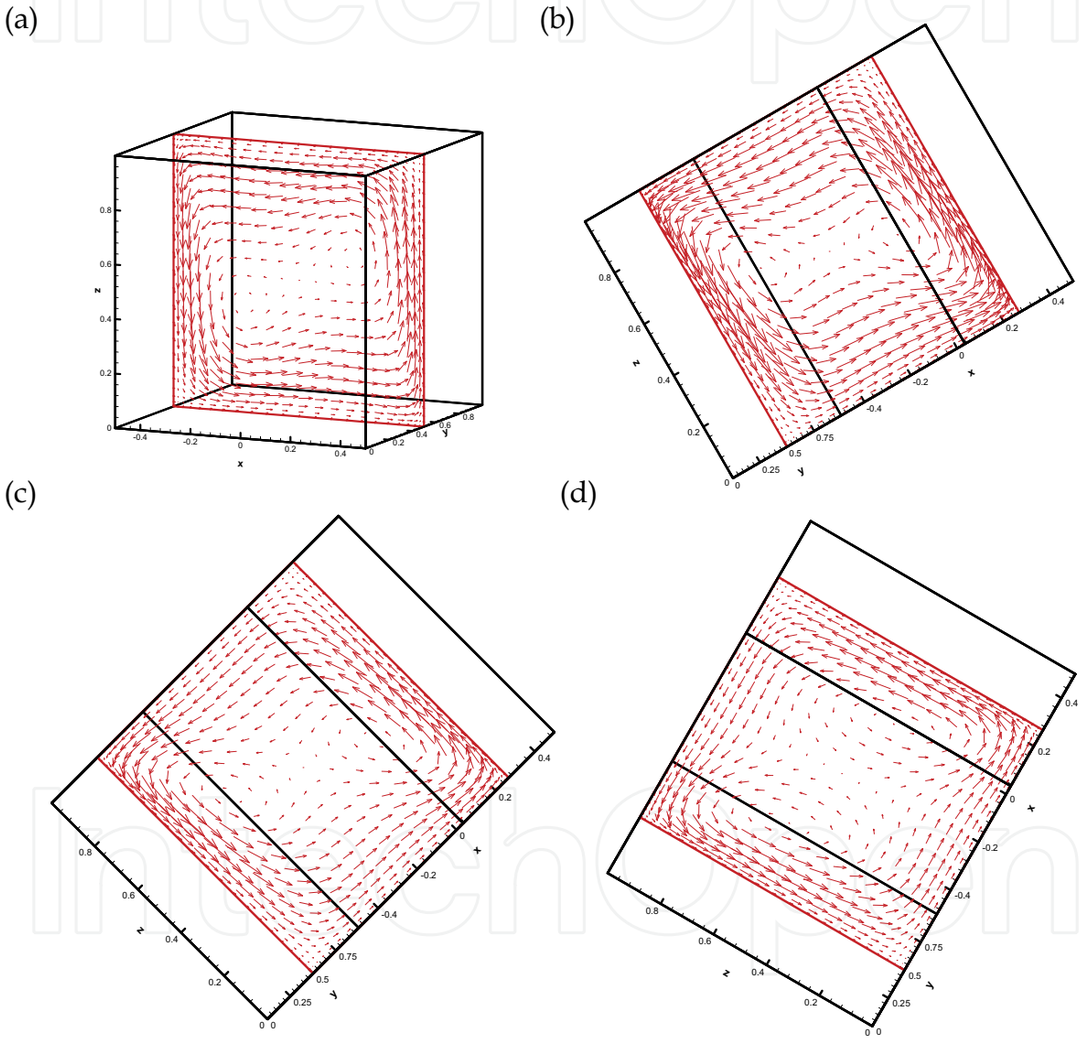

Fig. 3. Velocity vectors at $y=0.5$ plane for $Ra=10^5$ in a different angle (a) $\phi=0^0$ (b) $\phi=30^0$ (c) $\phi=45^0$ (d) $\phi=60^0$

The capability of the present numerical scheme can be tested by plotting the vorticity contours at the $y=0.5$ plane as shown in Figure 4 for different angles of inclination for

$Ra = 10^5$. As the angle of inclination increases, the buoyancy force is not sufficient enough to generate the convective current of the fluid. Hence the expected increased fluid convection due to decrease in the angle of inclination.

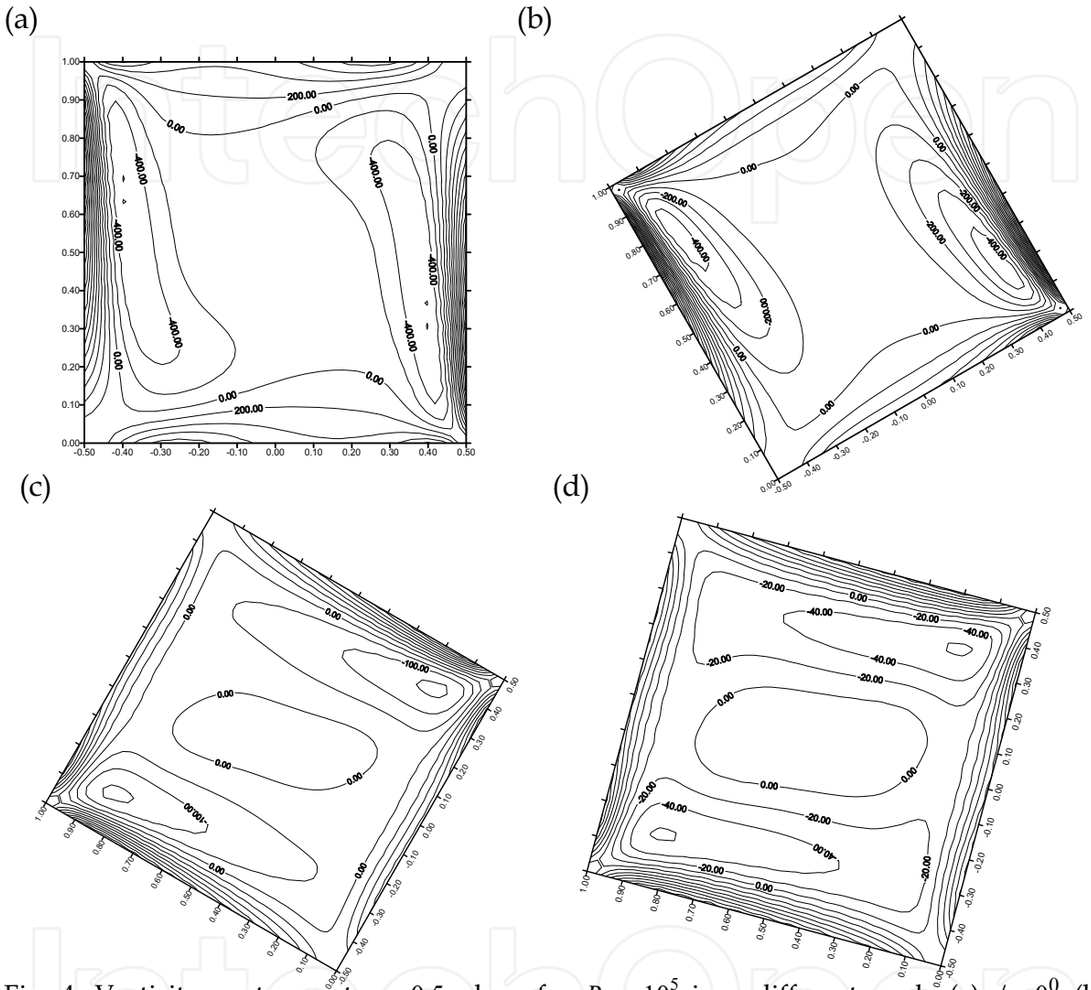

Fig. 4. Vorticity contours at $y = 0.5$ plane for $Ra = 10^5$ in a different angle (a) $\phi = 0^0$ (b) $\phi = 30^0$ (c) $\phi = 60^0$ (d) $\phi = 75^0$

Nusselt number is an important non-dimensional parameter in convective heat transfer study. The mean value of the Nusselt number computed for the isothermal walls are shown as variations along the $y-$ direction in Figures. 5(a) to 5(d) for $Ra = 10^3, 10^4, 10^5, 10^6$ respectively. An initial look on the range of the Nusselt number values shown on these figures clearly indicates that the Nusselt number increases with increase in the value of the Rayleigh number as expected. A symmetric variation is observed in all these figures. However the number of peaks and their positions vary with the value of the Rayleigh number. The maximum value of the Nusselt number is achieved only for $\phi = 0^\circ$ as expected.

As the angle of inclination increases, the maximum value of the Nusselt number decreases as seen from these figures for the cases of $Ra = 10^3, 10^4, 10^5, 10^6$.

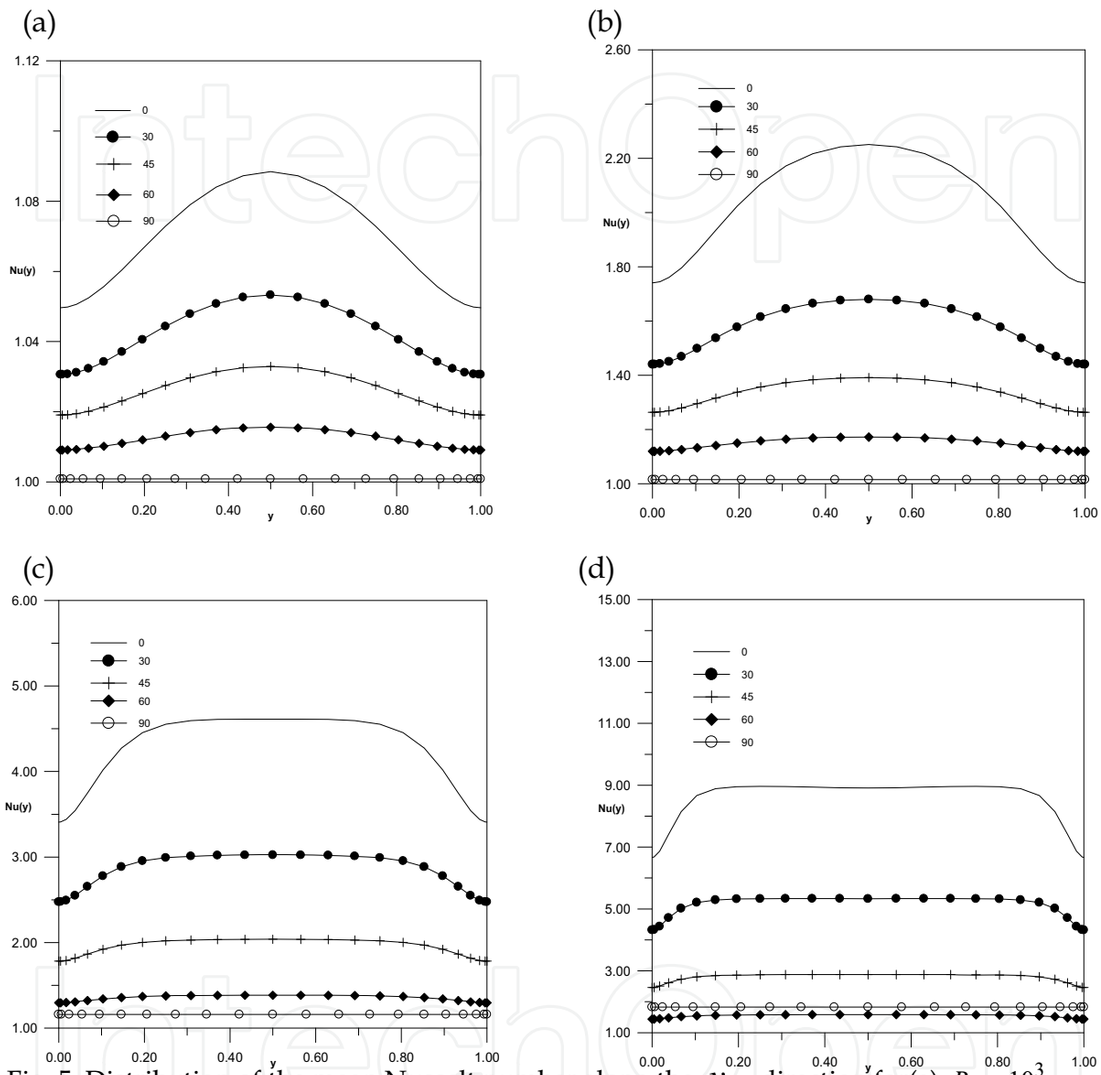

Fig. 5. Distribution of the mean Nusselt number along the $y-$ direction for(a) $Ra = 10^3$ (b) $Ra = 10^4$ (c) $Ra = 10^5$ (d) $Ra = 10^6$

The results discussed for the inclined cavity demonstrate that the present numerical algorithm has correctly predicted the convective heat transport process inside the cavity for different values of angle of inclination. The proposed algorithm could enforce the vorticity boundary values implicitly. This fact is verified by the expected results predicted by the present algorithm for the flow and the temperature fields.

6. Conclusion

The present study is extended to cover both 2D and 3D viscous flow models with demonstrated application to natural convection in a differentially heated inclined cavity, and we have achieved results with high accuracy. We can conclude with certainty that our differential quadrature/velocity-vorticity formulation are able to successfully simulate 2D and 3D natural convection problems. Test results obtained for Rayleigh number in the range from 10^3 to 10^6 at the angle of incidence ($\phi = 0^\circ$) show close agreements with other numerical scheme, producing the expected flow and temperature fields. The key issue in the salient characteristics of the different angle of incidence, $0^\circ \le \phi \le 90^\circ$ of natural convection in an inclined cavity are well-illustrated in the present study.

7. Acknowledgment

The support under Grant NSC 96-2221-E-022-014 by the National Science Council of Taiwan is gratefully acknowledged.

8. References

Fasel, H. (1976). Investigation of the stability of boundary layers by a finite-difference model of the Navier-Stokes equations, *J. Fluid Mech.*, 78, pp. 355-383.

Bellman, R. E.; Kashef, B.G. & Casti, J. (1972). Differential quadrature: a technique for the rapid solution of nonlinear partial differential equations, *J. Comput. Phys.*, 10, pp. 40-52.

Shu, C. & Richards, B. E. (1992). Application of Generalized Differential Quadrature to Solve 2-Dimensional Incompressible Navier-Stokes Equations, *International Journal for Numerical Methods in Fluids*, 15, pp. 791-798.

Shu, C. (2000). *Differential quadrature and its application in engineering*, Springer, London, 2000.

Lo,D. C.; Young, D. L. & Murugesan, K. (2005). GDQ method for natural convection in a square cavity using a velocity-vorticity formulation, *Numer. Heat Transfer, Part B*, 48. pp. 363-386.

Lo,D. C.; Young, D. L. & Murugesan, K. (2005). GDQ Method for Natural Convection in a cubic Cavity using a Velocity-Vorticity Formulation, *Numerical Heat Transfer B*, 48, pp. 363-386.

Tric, E.; Labrosse, G. & Betrouni, M. (2000). A first incursion into the 3D structure of natural convection of air in a differentially heated cubic cavity, from accurate numerical solutions", *Int. J. Heat Mass Transfer*, 43, pp. 4043-4056.

IntechOpen

Recent Advances in Technologies

Edited by Maurizio A Strangio

ISBN 978-953-307-017-9

Hard cover, 636 pages

Publisher InTech

Published online 01, November, 2009

Published in print edition November, 2009

The techniques of computer modelling and simulation are increasingly important in many fields of science since they allow quantitative examination and evaluation of the most complex hypothesis. Furthermore, by taking advantage of the enormous amount of computational resources available on modern computers scientists are able to suggest scenarios and results that are more significant than ever. This book brings together recent work describing novel and advanced modelling and analysis techniques applied to many different research areas.

How to reference

In order to correctly reference this scholarly work, feel free to copy and paste the following:

D. C. Lo (2009). DQ Analysis of 2D and 3D Natural Convection in an Inclined Cavity Using a Velocity-Vorticity Formulation, Recent Advances in Technologies, Maurizio A Strangio (Ed.), ISBN: 978-953-307-017-9, InTech, Available from: http://www.intechopen.com/books/recent-advances-in-technologies/dq-analysis-of-2d-and-3d-natural-convection-in-an-inclined-cavity-using-a-velocity-vorticity-formula

INTECH
open science | open minds

InTech Europe
University Campus STeP Ri
Slavka Krautzeka 83/A
51000 Rijeka, Croatia
Phone: +385 (51) 770 447
Fax: +385 (51) 686 166
www.intechopen.com

InTech China
Unit 405, Office Block, Hotel Equatorial Shanghai
No.65, Yan An Road (West), Shanghai, 200040, China
中国上海市延安西路65号上海国际贵都大饭店办公楼405单元
Phone: +86-21-62489820
Fax: +86-21-62489821

IntechOpen